FABRICATION AND CHARACTERIZATION OF HYBRID COLLOIDAL SILICON CARBIDE QUANTUM DOTS ON NANOSTRUCTURED SILICON FOR PHOTOVOLTAIC APPLICATION

OLAOYE ABDULMUTOLIB OLAJIDE

UNIVERSITI SAINS MALAYSIA

2025

FABRICATION AND CHARACTERIZATION OF HYBRID COLLOIDAL SILICON CARBIDE QUANTUM DOTS ON NANOSTRUCTURED SILICON FOR PHOTOVOLTAIC APPLICATION

by

OLAOYE ABDULMUTOLIB OLAJIDE

Thesis submitted in fulfilment of the requirements
for the degree of
Doctor of Philosophy

February 2025

ACKNOWLEDGEMENT

I am thankful to the Almighty Allah for the PhD journey He has bestowed upon me. I would like to express my sincere gratitude to everyone who have extended their assistance, support, and companionship throughout the journey and towards the completion of my thesis. Foremost, I am grateful and indebted to my committed and dedicated supervisor, Dr Mohd Marzaini Mohd Rashid who was always there, providing guidance, support, and motivation. Words alone cannot express my gratitude for all that he has done. I would like to thank my co-supervisors, Prof. Md. Roslan Hashim and Associate Prof. Mohd Zamir Pakhuruddin for their kind suggestions and help in this research work. I would like to thank Associate Prof. M. Hazwan Hussin, Dr Siti Azrah Mohamad Samsuri and Dr Mahayatun Dayana Johan for their kindness in helping me with the electrochemical measurements and suggestions during research work.

Much of this work would not have been possible without the technical support from the technical staffs of Nano-Optoelectronics Research (NOR) Laboratory. Some of them to mention are Mrs. Aznorhaidal Ramli, Mr. Abdul Jamil Yusuf and Mr. Yushamdan Yusof. I am thankful to my colleagues, Dr Sani Muhammad, Asad, AbdulAzeez Hayatu, Shehu Yusuf, Sameen Aslam, Shawbo Abdulsamad Abubaker, Saleh K. Alsaee, Elham Mzwd, Sani Saleh, Suleman Kazim Omotayo, Maryam Nike Abdul-Raheem, Ajetumobi Rukayat, Efenji Godwin Irinam, Usman Abdulkareem. My appreciation and word of thanks also goes to my colleagues, Dr Usman Muftau, Dr Olabomi Olaosebikan Ebenezer, Dr Adeyemi Kemi, Olawale Kazeem, Wasiu Ibrahim and Adeolu Babawale at Science Technology Department, Federal Polytechnic Offa and many more who have contributed and made my years in pursuing PhD interesting

as it was challenging. I would like to express my heartfelt gratitude to my uncles, Chief G.G. Jaiyeola and Mr Olaoye Muftau Boda extending their generous hospitality and kindness to my family back home. I would like to thank my cousins, Shola Jaiyeola, Dr Ganiyat Salawu, Nasiru Salawu, Olaoye Yusuf Opeyemi, Ganiyat Olaoye and Olaoye Sharafadeen for their encouragement. I am indebted to both Federal Polytechnic Offa and the Tertiary Education Trust Fund (TETFUND) for sponsoring my study through the AST&D scholarship. To my wife Kudirat, my children Halimah, Yusuf, and Mohd' Nabeel, my parents and family members, thank you for your great patience, motivation and unwavering support throughout my PhD program.

TABLE OF CONTENTS

LIST OF TABLES

Page

LIST OF FIGURES

Page

LIST OF SYMBOLS

d	Absorber Thickness
α	Absorption Coefficient
$S(\lambda)$	AM1.5G Solar Spectrum
E_g	Bandgap
Φ_{SBH}	Barrier height
θ	Bragg's angle
V_{bi}	Build-in potential
ρ	Concentration of etchants
D	Crystallite size
J_{sc}	Current density of cathodic process
J_D	Dark current density
^oC	Degree Celsius
E	Electric field
e	Electron
Ea	Electron affinity
n_e	Electron carrier concentration
μ_e	Electron carrier mobility
Ns	Electron Density
v	Electron velocity
eV	Electron volt
υ	Frequency
R_h	Hall coefficient

LIST OF ABBREVIATIONS

AZO	Aluminum Doped Zinc Oxide
Al_2O_3	Aluminum Oxide
ARCs	Antireflection Coatings
AFM	Atomic Force Microscope
ALD	Atomic Layer Deposition
b-Si	Black Silicon
b-Si nanowires	Black Silicon Nanowires
BZO	Boron Doped Zinc Oxide
CSCs	Carrier Selective Contacts
$CuAl_x$	Chalcopyrite
CB	Conduction Band
CPD	Contact Potential Difference
c-Si	Crystalline Silicon
DI H_2O	Deionized Water
DOS	Density of States
DMSO	Dimethyl Sulfoxide
DC	Direct Current
DASH	Dopant-Free Asymmetric Hetero-Contacts
NPs	Nanoparticles
OLEDs	Organic Light-Emitting Diodes
PL	Photoluminescence
PV	Photovoltaic
PVMD	Photovoltaics Materials and Devices
PCE	Power Conversion Efficiency
RCA	Radio Cooperation of America
RF	Radio Frequency
RIE	Reactive Ion Etching
RMS	Root Mean Square
c-Si	Silicon
$HAuCl_4$	Tetra Chloroauric Acid
TMAH	Tetramethylammonium Hydroxide

Sn	Tin
TiO_2	Titanium Oxide
TMO	Transition Metal Oxides
TCO	Transparent Conductive Oxides
WO_3	Tungsten Trioxide
UV-Vis-NIR	Ultraviolet Visible Near Infrared
VB	Valence Band
V_2O_5	Vanadium Pentoxide
H_2O	Water
WAR	Weighted Average Reflectance

FABRIKASI DAN PENCIRIAN TITIK KUANTUM HIBRID KOLOID SILIKON KARBIDA ATAS SILIKON BERSTRUKTUR NANO UNTUK APLIKASI FOTOVOLTA

ABSTRAK

Silikon karbida (SiC) adalah salah satu bahan semikonduktor yang paling berpotensi untuk optoelektronik kerana sifat unggulnya seperti ketahanan tinggi terhadap kemerosotan kimia, elektrik dan optik. Nanopartikel semikonduktor yang lebih kecil daripada 10 nm telah menunjukkan sifat fizikal dan kimia yang bergantung pada saiz. Nanopartikel SiC dalam julat saiz 1-6 nm menjadi tumpuan dalam pelbagai bidang seperti optoelektronik, fotovolta, optik kuantum, bioimej, dan diagnostik perubatan, kerana sifat kefotopendarcahayaan yang dipertingkatkan. Dalam aplikasi fotovolta, penggunaan titik kuantum (QDs) 3C-SiC koloid belum sepenuhnya direalisasikan sebagai penukar-turun, untuk memulihkan kehilangan foton yang diserap akibat kehilangan termalisasi. Dalam kerja ini, QDs 3C-SiC koloid yang disintesis menunjukkan saiz zarah dalam julat saiz kurungan kuantum dan peningkatan kefotopendarcahayaan serta penyerapan dengan peralihan Stokes sebesar ~277 nm (4.48 eV), yang disebabkan oleh pengurangan saiz zarah yang lebih kecil daripada diameter Bohr eksiton (4 nm) 3C-SiC pukal. Peralihan Stokes yang besar adalah petunjuk bahan penukar-turun yang baik. Penyerapan jalur lebar silikon kristal (c-Si) diperbaiki melalui teknik punaran kimia yang dibantu logam yang mengurangkan pantulan jalur lebar c-Si. Untuk menyiasat kesan fotokonduktif QDs, hibrid koloid 3C-SiC/b-Si dengan fotokonduktiviti yang dipertingkatkan disintesis untuk kepekatan QDs yang berbeza (9, 12 dan 15 mg/mL). Peningkatan dalam fotokonduktiviti peranti adalah disebabkan oleh kesan penukar-turun QDs. Selain itu, sel suria dengan

kecekapan penukaran kuasa (PCE) 7.04 % untuk kepekatan 12 mg/mL QDs 3C-SiC koloid pada substrat b-Si yang disepuh lindap pada 400˚C dicapai. Apabila suhu sepuh lindap dinaikkan kepada 600˚C untuk rawatan pasca-metalisasi, ia menunjukkan PCE yang dipertingkatkan sebanyak 10.44 %. Selain itu, 9 mg/mL 3C-SiC juga menunjukkan PCE yang dipertingkatkan sebanyak 8.59 % apabila disepuhlindap pada 600˚C. Untuk menyiasat lebih lanjut kesan penukaran-turun 3C-SiC koloid, QDs dititis pada sentuhan hadapan sel suria, menghasilkan PCE sebanyak 9.75 %. Oleh itu, QDs 3C-SiC koloid telah menunjukkan kesan penukar-turun, di mana cahaya UV diserap oleh QDs dan dipancarkan semula ke dalam tenaga foton yang boleh dilihat untuk diserap oleh pengesan b-Si yang mendasari, mengakibatkan pengurangan rekombinasi pembawa cas. Prestasi keseluruhan sel suria yang dihasilkan adalah disebabkan oleh kesan penukaran-turun QDs 3C-SiC koloid.

FABRICATION AND CHARACTERIZATION OF HYBRID COLLOIDAL SILICON CARBIDE QUANTUM DOTS ON NANOSTRUCTURED SILICON FOR PHOTOVOLTAIC APPLICATION

ABSTRACT

Silicon carbide (SiC) is one of the most promising semiconductor materials for optoelectronics owing to its superior properties such as high resistance to chemical, electrical and optical degradation. Semiconductor nanoparticles smaller than 10 nm have shown size-dependent physical and chemical properties. SiC nanoparticles in the size range of 1-6 nm are in the centre of interest in wide-ranging areas such as optoelectronics, photovoltaics, quantum optics, bioimaging, and medical diagnostics, owing to its enhanced luminescent properties. In photovoltaic application, the use of colloidal 3C-SiC quantum dots (QDs) has not been fully realized as a down-convertor, to recover the absorbed photon loss due to thermalization loss. In this work, the synthesized colloidal 3C-SiC QDs exhibit particle size in the quantum confinement size range and enhanced photoluminescence and absorbance with large Stokes shifts of ~277 nm (4.48 eV), which is due to the decrease in particle size smaller than the exciton Bohr diameter (4 nm) of bulk 3C-SiC. The large Stokes shift is an indicative of good down-converting material. The broadband absorption of crystalline silicon (c-Si) is improved via the metal-assisted chemical etching technique which decreases the broadband reflection of the c-Si. To investigate the photoconductive effect of the QDs, hybrid colloidal 3C-SiC/b-Si with enhanced photoconductivity is synthesized for different concentrations of QDs (9, 12 and 15 mg/mL). The enhancement in the device's photoconductivity is due to the down-conversion effect of the QDs. Furthermore, solar cells with power conversion efficiency (PCE) of 7.04 % for 12

mg/mL concentration colloidal 3C-SiC QDs on b-Si substrate which was annealed at 400 ^{o}C is achieved. When the annealing temperature is increased to 600 ^{o}C for post-metallization treatment it shows an improved PCE of 10.44 %. Moreover, 9 mg/mL 3C-SiC also exhibits enhanced PCE of 8.59 % when annealed at 600 ^{o}C. To further investigate the down-conversion effect of the colloidal 3C-SiC, the QDs were drop-casted on the front contact of the solar cell, resulting in a PCE of 9.75 %. Consequently, the colloidal 3C-SiC QDs have demonstrated its down-conversion effect, where the UV light is absorbed by QDs and reemitted into the visible photon energies to be absorbed by the underlying b-Si detector resulting in reduced charge carrier recombination. The overall performance of the fabricated solar cells is attributed to the down-conversion effect of colloidal 3C-SiC QDs

CHAPTER 1

INTRODUCTION

1.1 Introduction

As the world is encountering an increase in energy demand, global warming, and depletion of fossil fuels, there is a need for renewable and clean energy sources. Photovoltaics (PV) is the conversion of sunlight into electricity, which offers a sustainable energy solution. In contrast to other power-generating technologies like nuclear and hydroelectric, among others, the adoption of PV technology has recently grown in popularity recently to ~3.6 % [1], [2]. PV is a substantial and rapidly growing green substitute for traditional fossil fuel electricity. From crystalline silicon to organic solar cells, tandem solar cells, and thin film solar cells, the solar cell business is growing rapidly. To lessen the impact of fossil fuel-induced global warming, efforts to boost the efficiency of photovoltaic (PV) technology and reduce the quantity of raw materials and manufacturing processes used in conversional crystalline silicon solar cells have gained attention. Three spectrum conversion methods such as down shifting, down conversion, and up conversion, have been introduced, and some researchers have examined the effects of these processes on various types of solar cells. According to Nanoscale magazine [3], this invention represents the third or next generation of solar cells.

Solar cells consist of materials that interact with light. When incoming is incident on semiconductor solar cells, one of the four predicted reactions is produced, as shown in **Figure 1.1**. In particular, it produces electron-hole pairs upon absorption of photons with energies larger than the semiconductor bandgap, producing free carriers that allows the electrons to move around the circuit as a direct current upon carrier separation and collection. This is how solar cells create electricity. However,

photons with energies lower than the semiconductor bandgap energy are not absorbed but are transmitted. In addition to the known surface reflection that may occur on each material edge, there is a likelihood that the excited electron recombines with the hole. This process can be either radiative or more commonly, non-radiative recombination, which results in recombination losses. The beam in **Figure 1.1** represents the properties of light such as reflection, absorption, scattering, and transmission that will be discussed. Surface reflection occurs at the cell front and rear edges. Additionally, specular reflection which occurs when light strikes a cell at an angle different from the surface normal, can result in reflection [3].

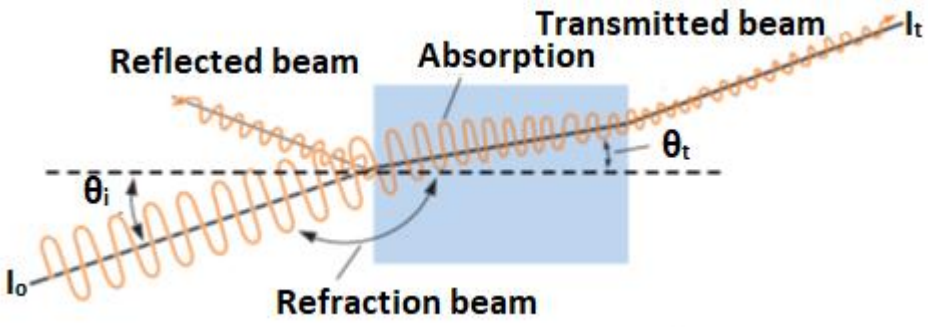

Figure 1.1 Interaction of Light with Solar Cell Material [3]

1.2 Solar Cell Issues and Limitations

The solar cell's output is restricted by multiple loss mechanisms, which are as follows:

1.2.1 Loss From Non-Absorption of Long Wavelengths:

Photon with energy below the solar cell's band gap cannot produce an electron-hole pair; hence, longer wavelengths is not absorbed.

1.2.2 Loss as a Result of Thermalizing Photons' Excess Energy

When photons have energy above the band gap, they form "hot" electron-hole pairs, which eventually decay to the lowest energy state and release their excess energy through the thermalization of the material.

1.2.3 Loss from Reflection

Photon that are not available for conversion are a result of reflection from the solar cell's upper surface, which is caused by the cell's optical characteristics.

1.2.4 Loss as a Result of Partial Absorption Because of the Limited Thickness

The solar cell's absorption coefficient varies with wavelength and decreases as the wavelength increases. As a result, photon with energy close to the bandgap need a longer path length within the material to be absorbed and converted. A portion of the long-wavelength radiation escapes the cell because of its finite thickness, making it unavailable for conversion.

1.2.5 Recombination Loss

Electron-hole pair that is generated is unstable and must be collected at the electrodes within a specific decay time to either produce a photon or heat in the material. Additionally, the presence of defects in the material facilitates recombination, which lowers the cell's power output.

1.2.6 Losses Due to Shading Losses and Metal Electrode Coverage

There is metal electrode coverage in the top surface of the front contact of the solar cells, which obstructs the incoming incident light by reducing the amount of electricity being generated.

1.2.7 Voltage Factor Loss

Due to the fundamental recombination, which is dependent on the material's electronic quality and doping concentration, the V_{oc} of the solar cell is less than the band gap energy, which results in a lower conversion efficiency.

1.2.8 Loss From Fill Factor

The solar cell's efficiency is further decreased by the presence of series and shunt resistances, which causes loss in the fill factor indicating the reducing in the maximum power to be generated. The losses for a c- Si solar cell with 15% commercial efficiency are shown in **Figure 1.2**.

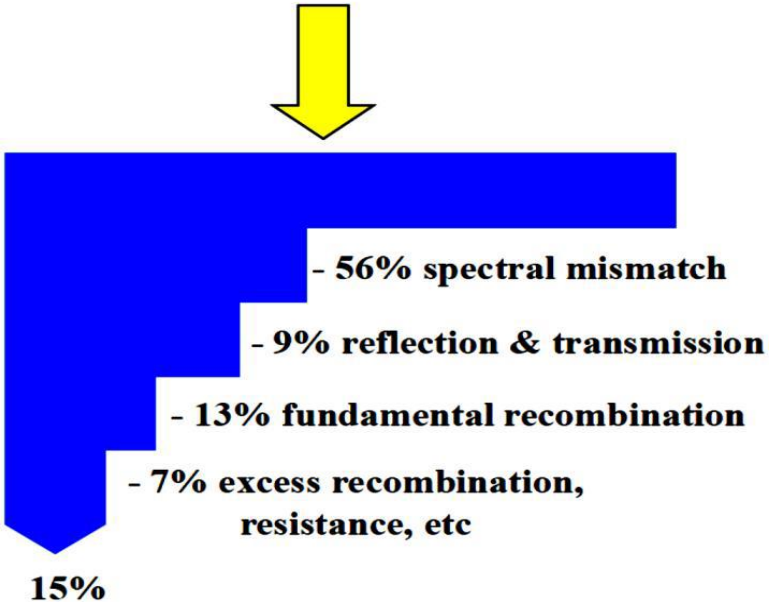

Figure 1.2 Losses in a Commercial C-Si Solar Cell With 15% Efficiency Spectral Mismatch, Reflection & Transmission, Fundamental Recombination, Excess Recombination, And Resistance [4]

The loss as a result of photon thermalization and losses from reflection will be the major focus in this work in order to increase the photoconductive and absorption of the fabricated solar cell.

1.3 Background of Nanostructured Silicon

Crystalline silicon (c-Si) solar cells have dominated ~90 % of the PV market owing to its mature manufacturing technology, long-term stability, and non-toxicity of the material. Furthermore, c-Si is the second most abundant element in Earth-crust and has proven to be a highly attractive solar absorber. Despite appealing advantages such as low-cost and long lifetime, c-Si solar cells suffer from weak absorption coefficient, which is attributed to the indirect bandgap nature of c-S. The absorption coefficient of the c-Si can be increased by nanotexturing the surface of c-Si [5], [6]. A c-Si surface with a variety of nanotextures and outstanding broadband light absorption from ultraviolet (UV) to infrared (IR) regions is known as black silicon (b-Si) [22]. The development of b-Si, which produce micro-spikes on the top surface of c-Si, was initially accomplished in 1995 by Jansen *et al*. via the reaction ion etching (RIE) approach [23]. The b-Si is black in appearance to the naked eye, as depicted in **Figure 1.3**, with a very low reflection of incident wideband light, which tends to give absorption of the incident light much efficiently [24,25]. Because of the improved light trapping and coupling caused by the graded refractive index at the air-silicon interface, which is attributed to the nanostructure's nature with lower dimensions relative to the wavelength of incident light, b-Si exhibits superior light absorption [24]. Owing to its low fabrication cost and wideband (300-1100 nm) light absorption characteristic, b-Si is being researched as a possible substitute for planar c-Si in a variety of applications (such as photovoltaics and photodetectors) [24,26,27].

To attain superior light trapping/coupling in the nanostructures on the b-Si surface, researchers have fabricated various forms, including nanowires [11], nanopillars [29], nanocones [30], nanopores [31], and nanograss [32]. The shape of the fabricated nanostructures is named without following any set rules. Some names for

comparable shapes are used interchangeably because it is merely a visual interpretation [33]. The b-Si exhibits numerous other exceptional qualities in addition to its exceptional broadband light absorption capability, including surface hydrophobicity, antibacterial surface, high aspect-ratio, and modified band structure. As a result, the b-Si exhibits exceptional qualities, making it a viable option for various applications, including photovoltaic cells [24,26], photodetectors [27], energy storage devices [36], biosensors [37], antibacterial surfaces [39], drug analysis [40], terahertz emitters [41]. However, due to effective light trapping/coupling in the nanohole/nanopore arrays, a benefit of using nanowire b-Si, the silicon nanoholes or nanopores (SiNHs or SiNPs) are mechanically robust and exhibit extremely low wideband light reflection property in contrast to the delicate and fragile free-standing silicon nanowires/nanopillars [34, 35]. The aim of this research project is to develop a technique for producing nanowire b-Si that is simple, affordable, and allows for precise control over nanopore morphology for photovoltaic applications.

The b-Si material is an excellent wideband light-absorbing material that does not require conventional anti-reflective coating (ARC). This lowers manufacturing costs and could be a great option for silicon-based PV cells with better performance in terms of cost-to-power conversion efficiency ratio [24].

Nonetheless, despite the low wideband reflection in b-Si, enhanced surface recombination of charge carriers (photogenerated electron-hole pairs) in the large surface area of the nanostructures b-Si provide a significant obstacle to the use of b-Si in PV cells and lead to low power conversion efficiency [24]. This problem in b-Si PV cells may be solved through photon energy down-conversion by placing high-quality, high-yield QDs on the top surface of the nanotextured b-Si by growing or depositing

a thin layer of QDs material such as lead sulfide (PbS), cadmium sulfide (CdS), Zinc sulfide and silicon carbide (SiC) [7]. The PbS colloidal solar cells have reported a efficiency of 2.1% [8] to 3 % with ternary PbS_xSe_{1-x} nanocrystals [9], [10]. The improvement in the efficiency was achieved through advance in the electronic properties of PbS colloidal nanocrystals by varying the particle size between 1 and 3 nm to give a power conversion efficiency of 4.6 % [11] At present, the highest efficiency obtained for colloidal quantum dot solar cells is 18.1 % [12]

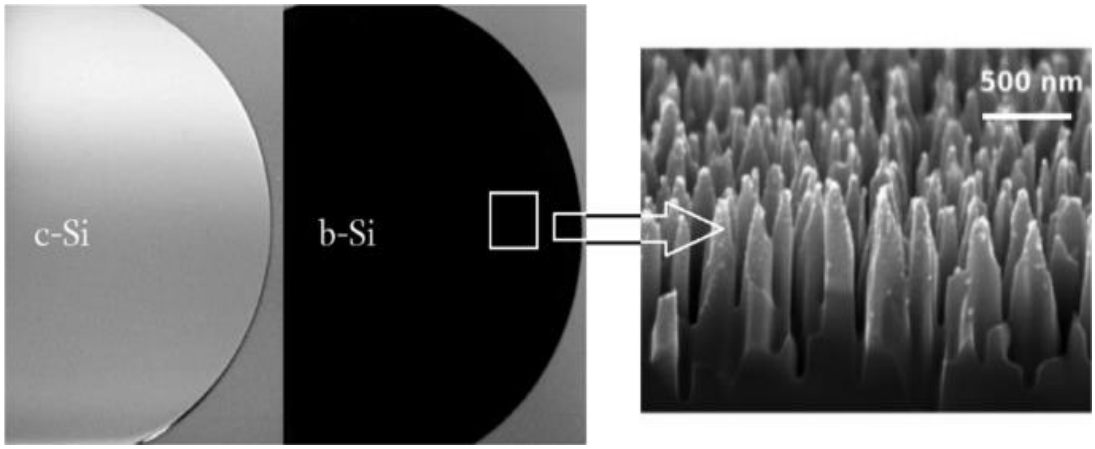

Figure 1.3 Appearance of (a) Planar c-Si (b) b-Si and (c) Nanowire after MACE etching

1.4 Research Motivation

With the increase in energy demand owing to the growth of the global population. The solar energy presents a renewable, clean, abundant, and sustainable solution to meet the growing energy demands. Silicon-based solar cells have dominated the PV market of about 95 % sales [13], [14] due to the abundance of Si material in the earth's crust, advanced technology, and cost-effectiveness. Despite these advantages, Si-based solar cell still suffers from a low absorption coefficient (3105 cm^{-1} at λ = 633 nm) and poor photon absorption of 60 % [15], [16], [17]. A lot

of work is being done to enhance the c-Si light absorption, which is essential for raising photocurrent in PV cells. One of the most popular PV industry standards is to use a quarter-wavelength dielectric material with a thick layer (e.g., SiO_x, SiN_x, Al_2O_3, ZnO, or a mixture of these) as an ARC to reduce the reflection (below 10 %) from the planar c-Si surface [18], [19], [20]. The incorporation of nanotextures on a planar c-Si surface (nanostructured b-Si) is another promising, cost-effective, and less restrictive method to reduce broadband light reflection. Without any ARC, this method produces an average light reflection that is even less than 5%. The refractive index grading effect, which causes incident light to be trapped in nanostructures with reduced dimensions relative to wavelengths that have a graded refractive index throughout their thickness (at least half the wavelength of the incident light), is responsible for the increased light trapping in the nanotextured surface of the planar c-Si [21], [22], [23], [24]. Comparing the nanostructured b-Si to an ARC, it also offers wider angle anti-reflective properties and wideband absorption (300-1100 nm) [21], [25]. The best light trapping in the visible range is attained if the depth/height of nanostructures/microstructures is 250 nm or more [26]. Light gets trapped when incident light enters a medium that has a graded refractive index because of either microstructures or nanostructures. However, the increased surface area of the nanostructures on planar c-Si causes higher surface recombination of charge carriers in the nanostructured b-Si. Also, the thermalization loss occurs at the surface due to surface defects, which reduce the efficiency of the solar cell. These can be mitigated by applying a QDs material that will serve as a down-converter layer to convert photon from UV to visible region as well as a passivation layer made of a wide bandgap SiC [6], [14], [27]. This will improve the absorption and photoconductivity of the device leading to enhanced value of power conversion efficiency.

1.5 Problem Statement

Currently, planar bulk Si solar cell exhibit high surface reflection losses affecting short-circuit current J_{sc} and efficiency, thus there is a need to reduce reflection by nanostructuring via metal assisted chemical method (MACE) to black Si (b-Si). However, b-Si have surface defects that results in high recombination losses especially for absorbed UV photons at the surface. Therefore, UV photon energy down-conversion to visible photons utilising SiC QDs through hydrothermal chemical etching in HF/HNO_3 is highly promising route to mitigate surface recombination losses by absorbing the incident photon, which will be reemitted and absorbed by the underlying Si for enhanced photocurrent generation.

The purpose of this study is to optimize the hydrothermal etching technique of bulk SiC to produce monodisperse distribution of colloidal SiC QDs with quantum confinement effect for photovoltaic applications. Colloidal quantum dots (QDs) potential candidates in optoelectronic and photovoltaic applications owing to their optical size-tunable emission wavelength, narrow spectral linewidth, and near-unity photoluminescence quantum yield. Lead (Pb) and cadmium (Cd) chalcogenides have been the most popular fluorescent QDs because of their well-established synthesizing processes and well-understood optical characteristics. Toxicity properties of Pb and Cd which can cause serious health challenges such as brain and tissue damage if it is exposed to the environment have made researchers to search for potential candidate that will serve as non-toxic alternatives. Silicon-based QDs, are being investigated as alternative to Cd and Pb-based QDs since it is not toxic and more resistant to oxidation in ambient air. Si QDs have poor solubility and unstable luminescence due to their oxidation susceptibility in air and water. However, SiC QDs, non-toxic with extremely stable photoluminescence preferable option for optoelectronics and photovoltaic due

to high quantum yield and quantum confinement effect. In this work, to get a high yield of SiC QDs, powdered SiC has been chosen over wafer since it is more challenging to control the morphology of the nanoparticles generated from wafer. Additionally, wet chemical etching has been chosen as the SiC QD production method due to the requirement for tiny sizes and monodisperse distributions of the generated quantum dots in photovoltaic applications. There are significant efforts in both academia and industry to achieve dramatic improvements in the performance of quantum photovoltaic cells over the past decade owing to the development of high-quality QDs and optimized device architectures.

The fabricated colloidal SiC QDs will be incorporated into nanostructured Si (b-Si) to limit the thermalization loss and surface recombination to enhance the efficiency of the b-Si via a down-conversion technique of solar spectrum.

1.6 Objectives

The main objectives of the research are as the following:

1. To characterize the optimized 3C-SiCQDs fabricated by hydrothermal chemical etching for enhanced optoelectronics and photon energy down-conversion properties.

2. To characterize the optimized b-Si fabricated by one-step metal assisted chemical etching for enhanced broadband absorption.

3. To evaluate the photoconductivity and power conversion efficiency (PCE) performance of fabricated solar cell with hybrid colloidal 3C-SiC/b-Si nanostructure.

1.7 Original Contributions

- Hydrothermal wet chemical etching gives colloidal 3C-SiC QDs with high PL and large stokes shift is investigated and optimized at 100 ^{o}C at 2 hours.

- Investigation of down-conversion nature of 3C-SiC QDs for solar cells applications.

- Understanding the effect of HOMO-LUMO gap of 3C-SiC QDs on its optical properties using cyclic voltammetry.

- The b-Si etching time is investigated and optimized for 30 minutes at room temperature with low broadband reflection.

- Study the impact of the 3C-SiC QDs concentration on the performance of hybrid colloidal 3C-SiC QDs/nanostructure b-Si PV.

1.8 Thesis Outlines

This thesis consists of five (5) chapters.

Chapter 1 briefly explains the motivations behind the research on hybrid colloidal SiC QDs/ nanostructured b-Si for solar cell applications. It also introduces the importance of the quantum confinement effect of QDs and its significance in energy spectrum conversion for solar cells. The problem statement and research objectives are also highlighted in this chapter.

Chapter 2 includes the review of relevant literature and theoretical background information of QDs and solar cell fabrications. The reviewed related literature on Si QDs, SiC QDs, and its advantages over Si QDs, SiC polytype are

highlighted. Additionally, the light trapping in conventional c-Si solar cells right and one-step MACE approaches to incorporate nanostructure b-Si into c-Si solar cells are included. The general principles and theories of b-Si light-trapping properties for applications in solar cells are discussed. At the end of the chapter, possibilities of incorporating colloidal SiC QDs into nanostructure for hybrid colloidal 3C-SiC QDs/nanostructure b-Si solar cell are also presented.

Chapter 3 outlines the fabrication of colloidal SiC QDs via hydrothermal chemical etching method and one-step MACE method for b-Si, equipment, and procedure (flowchart) used for the fabrication of hybrid colloidal 3C-SiC QDs/b-Si PV cells. In the process of developing hybrid colloidal 3C-SiC QDs/b-Si and PV cells, this chapter also provides a brief explanation of the fundamental concepts underlying the tools used for cutting, deposition, thermal annealing, and characterization or measurement.

Chapter 4 presents the results of colloidal 3C-SiC QDs that include effect of etching parameters (temperature, time and concentration) on the fabrication of the device and nanostructured b-Si from one-step MACE including the effect of process parameters on b-Si formation. The optical, photoluminescence and electrochemical properties of colloidal 3C-SiC were optimized. Absorption achieved in the b-Si nanowires and hybrid colloidal 3C-Si QDs/b-Si surfaces compared to reference Bare Si and c-Si with QDs are investigated and discussed. Besides, the chapter presents morphological optical, and electrical properties of hybrid colloidal 3C-SiC QDs/b-Si and hybrid colloidal 3C-SiC QDs/c-Si interfaces. The optimum electrical parameters of the fabricated hybrid colloidal 3C-SiC/nanostructured b-Si solar cells are also presented in this chapter.

Chapter 5 summarises the experimental findings, highlights the novel contributions made to the study, and suggests more research related to this work.

CHAPTER 2

LITERATURE REVIEW

2.1 Introduction

Research on QDs has advanced significantly since their experimental discovery in the 1980s, and they are now used in various applications, including bioimaging, optoelectronics, and photovoltaic devices. However, before their potential can be fully realized in many fields, there is a need to replace the toxic materials present in most common QDs such as Cd/Pb-based QDs. Si QD was also explored as a replacement because it is a non-toxic material, but Si-based QDs exhibit weak luminescence and are also prone to oxidation, however, SiC QDs is discovered to be an excellent candidate because of its higher ambient stability and stable luminescence. Several techniques were explored in fabricating SiC QDs, such as stain etching and electrochemical etching. Amongst the techniques, wet chemical etching is considered a simple and effective method.

The quantum size effect in zero-dimensional nanometre-sized semiconductors was initially identified by the teams of Ekimov and Efros in the USSR [2] and Louis Brus and his colleagues at Bell Laboratories in the USA [3]. Murray, Norris, and Bawendi introduced the use of the hot-injection method, a high-temperature organometallic procedure in 1993, which paved way for the production of very homogeneous colloidal CdSe QDs [28], [29]. When Dabbousi and colleagues reported the synthesis of the core/shell structure that solved the issue photostability, which produced a 50% quantum yield [30]. The first water-soluble QDs that could be applied for labelling were published the following year [32]. Most researched QDs that have been studied widely are indium phosphide (InP) and indium arsenide (InAs) [32],

cadmium selenide (CdSe) and cadmium telluride (CdTe) [33], and lead selenide (PbSe) and lead sulfide (PbS) [34], [35]

Through altering the core/shell materials, the QDs' PL spectra can be tuned from the UV to the near-infrared (NIR) regions as seen in **Figure 2.1 (a)**. For instance, some QDs such as CdS, CdSe, InP, CdTe, and PbS with 2.5 nm in diameter exhibit near visible to NIR band-edge absorption. **Figure 2.1 (c**) depicts the quantum confinement effect, or the size-dependent emission of QDs [36]. In order to decrease the surface deficiency and boost the quantum yield, these typical QDs were conventionally synthesized as a core enclosed in a shell by large energy gap semiconductor, such as zinc sulfide (ZnS) as depicted in **Figure 2.1 (b)** [30], [37]

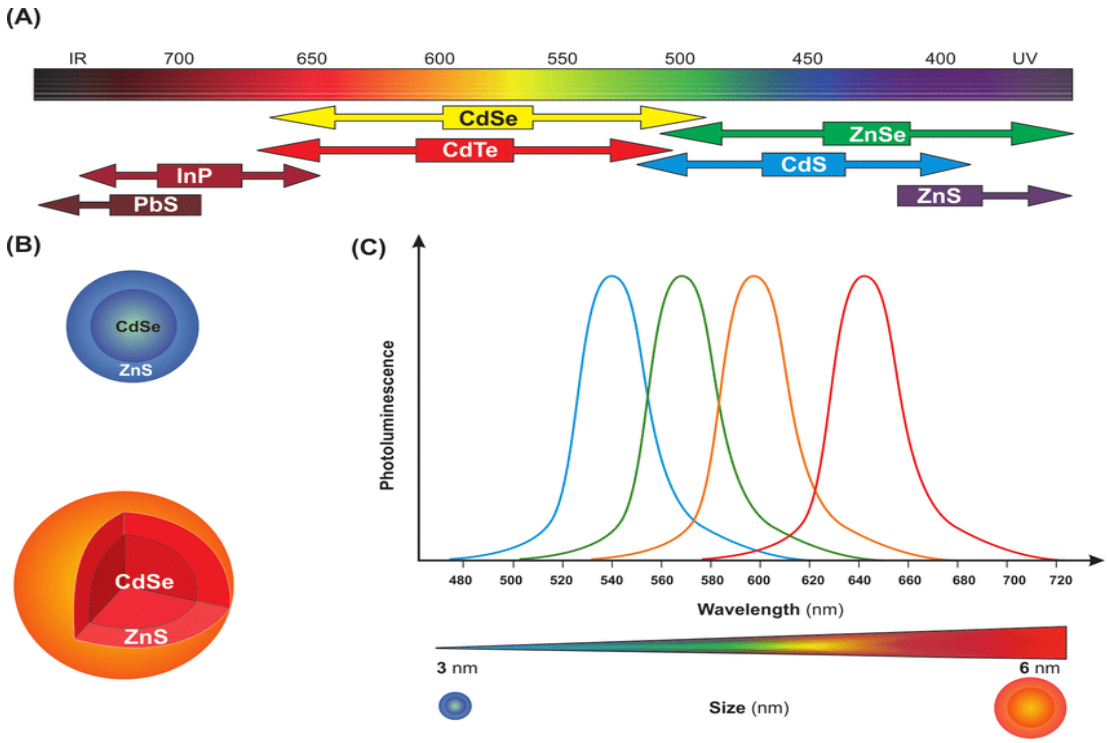

Figure 2.1 Schematic Representation of Different Types of QDs. (a) Various QDs and their Optical Spectra. (b) Structure of CdSe/ZnS QDs Core (c) Emission Spectra of Monodispersed CdSe/ZnS QDs. Note: not Drawn to Scale [36]

The uniqueness of quantum dots is the tunable physical properties and quantum confinement effect by the distinction of size and shape that is quite different from the

properties of bulk crystalline solids. For instance, in CdS with particle size below 10 nm, the band gap can be tuned between 2.5 eV and 4 eV by decreasing the size of spherical-shaped CdS nanocrystals [38]. **Figure 2.2** demonstrates such a quantum confinement effect.

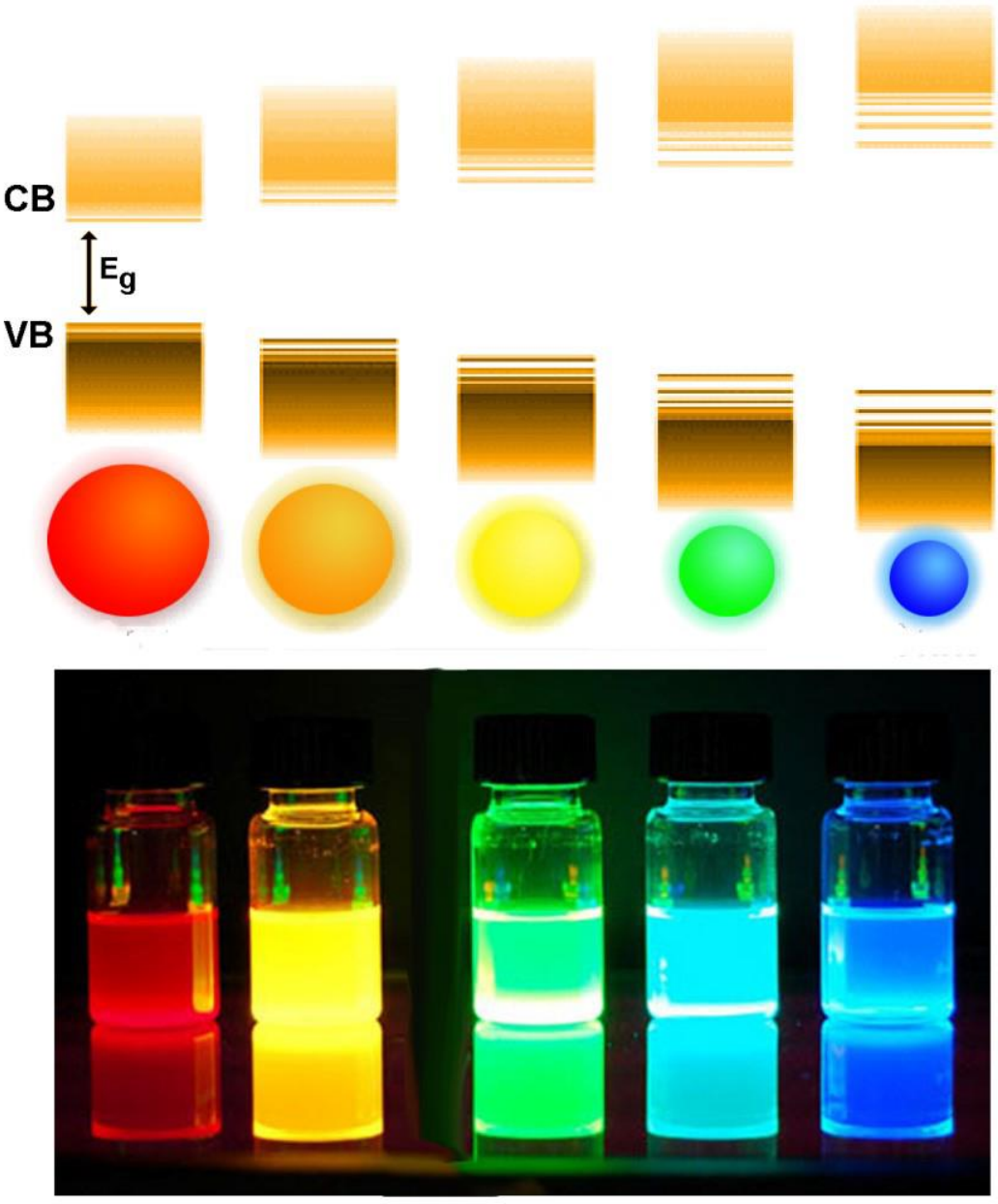

Figure 2.2 Quantum Confinement: The Smaller the Size of a QD, the Shorter the Emitted Color [39]

There are two families of quantum dots: colloidal quantum dots, which are solution-processed semiconductor nanocrystals with a size-tunable bandgap [40] and epitaxial quantum dots that are defined by electrostatic gates on substrates [41]. Epitaxial QDs can be referred to as layer-by-layer heterostructures monocrystalline films in nanoscale [42]. However, this report (thesis) only focuses on colloid QDs made from nanocrystals because it may be worth to comparing their costs of fabrication as colloidal QDs are much cheaper than epitaxial QDs which involve ultrahigh vacuum equipment such as molecular beam epitaxy machines that require expensive high-purity materials [43].

2.2 Silicon QDs

Silicon (Si) is an abundant and non-toxic element with little environmental impact and is a good replacement for Cd/Pb based QDs in optoelectronics and bioimaging applications. Although Si exhibits a low photoluminescence when it is in its bulk form due to its indirect bandgap, it offers increased optical characteristics at the nanoscale (QDs), which make Si an excellent candidate in a variety of fields, including electronics and medical [45], [46], [47]. Si QDs with sizes comparable to bulk Si with an exciton Bohr radius of about 4.2 nm, have shown a strong quantum confinement effect [47]. Si QDs have also been incorporated onto black silicon (b-Si) as a hybrid nanostructure for reflectance reduction over a wide range of broad spectrum (300-1000 nm). Also, incorporating Si QD onto the b-Si nanostructure exhibited a reflectance reduction at a wavelength of 600 nm from 9.9% to 6.5%. The decrease in reflectance can be attributed to refractive index matching and optical confinement of the Si QDs within the Si nanostructure, resulting in enhanced photocurrent owing to photon down-conversion (UV to visible) characteristic of Si QDs [6]. Teng *et al*., also reported the

fabrication of luminescent colloidal silicon quantum dots (Si QDs) based light-emitting diodes (LEDs). Si QDs LEDs with a narrow spectral linewidth of 23 nm and spectral stability from +4V to +8V were fabricated [48].

The method to fabricate Si QDs include electrochemical etching[6], [49], [50] laser ablation in liquids [51], [52], [53] solution-phase or wet chemistry methods [54], [55], [56], and atmospheric pressure plasmas [44].

The main challenges in Si QDs applications are unstable photoluminescence, prone to oxidation in air, and poor solubility in aqueous solution and water [46], [57]. To protect the Si cores, Si QDs are usually fabricated in nonpolar solvents with hydrophobic ligands on their surface, resulting in Si QDs with low solubility. Thus, this can be achieved through surface passivation and hydrophilic molecule attachment (organic ligands) of Si QDs which result in Si-C surface-bond capping that prevents Si-C surface bond from being oxidized and the same time makes it soluble in water [34], [58], [59]. Warner et al. reported the fabrication of water-soluble Si QDs by covering them with poly (acrylic acid) or allylamine [57]. Also, surface functionalization via the encapsulation of Si QDs with PEGylated micelle [46]. Recently, water-soluble Si QDs with considerable PL in the visible region spectrum, which was fabricated for biomedical applications via one-pot synthesis at room temperature. The Si QDs were capped with hydroxide, making it water-soluble with PL emission at 470 nm and quantum yields of 6 % [60]. The thermally fabricated Si QDs through hydrosilylation of 10-undecanoic acid on hydrogen terminated surface provided by thermal disproportionation of triethoxysilane hydrolyzed at pH 3, which followed by hydrofluoric etching show high molecular coverage of the surface monolayers, the bright light emission with high PL quantum yields (PLQYs), the long-term stability in

the PL property for monitoring cells, the reduced toxicity to the cells, and the high photothermal response are all characteristics of fabricated carboxy-terminated Si QDs that exhibit high solubility in water [61].

2.3 Silicon Carbide QDs

Silicon carbide (SiC) is a wide bandgap semiconductor with excellent optical, physical, and electronic properties. It may serve as an alternative material to replace Cd, and Pb, which are very toxic with the presence of heavy metals such as CdSe, PbS, and CdZnS [92] and outperformed Si in high temperature, high-frequency microelectronics, and high-power device application owing to its ability to withstand harsh environment, good mechanical strength, and high chemical resistance [93], [94]. However, bulk SiC like its Si counterpart is an indirect bandgap semiconductor with low photoluminescence (PL) quantum yield but SiC quantum dots (QDs) has shown strong yellow-to-blue PL with crystallite decreased close to or below exciton Bohr diameter, which can be attributed to quantum confinement effect [94]. Unlike Si QDs, SiC QDs possess strong Si-C bonds, which prevent the surface from being oxidized by giving it chemical stability owing to the strength of the Si-C bonds that does not change with size, thus surface passivation is not necessary after SiC QDs etching [65], [97], [98]. The interest in colloidal SiC QDs lies in their stability in different solvents (such as water, toluene, and ethanol) asides from being chemical, and oxidation resistant, colloidal SiC QDs retains their luminescent properties that are uniformly dispersed in solutions after storage in air over a long period (90 days) without surface passivation [99]. Additionally, a remarkable 17 % quantum yield was reported, comparable to what was observed in Si QDs [98]. SiC QDs suspended in water typically exhibit PL spectra with peaks spanning from around 300 nm to 600 nm, and the wavelength intensities

exhibit dependency with excitation. The suspension can typically be excited up to 500 nm, with excitation between 320 and 370 nm yielding the maximum emission intensity [97], [100]. **Figure 2.3** shows an example of PL spectra.

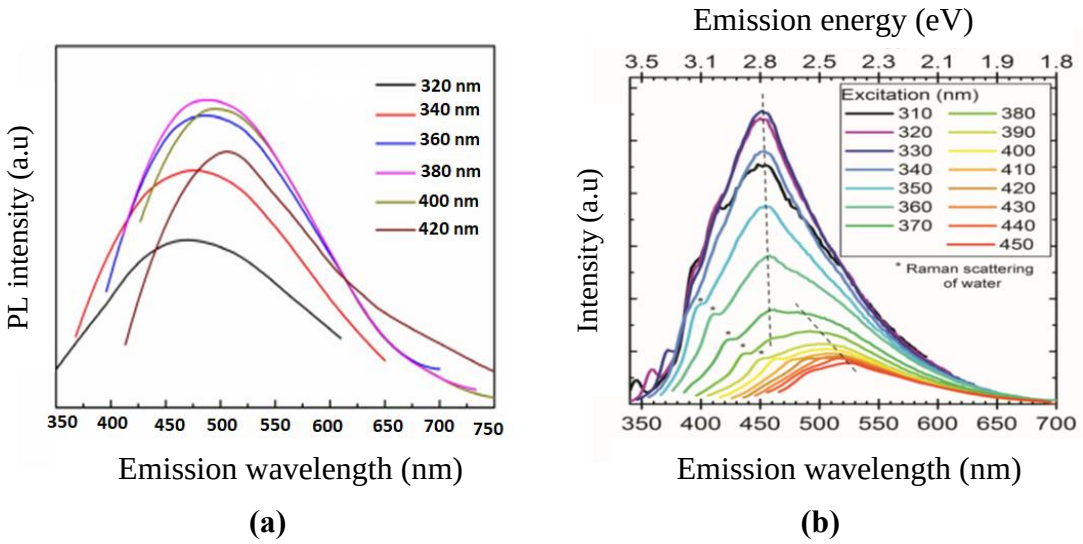

Figure 2.3 Photoluminescence Spectra of Colloidal SiC QDs (a) Dispersed in Ethanol [62] and (b) Dispersed in Deionized (DI) Water [63] at Different Excitation Wavelengths

The quantum confinement effect [64], [65], [66] and surface states [67], [68] are the radiative paths that are responsible for the PL emission. The quantum confinement effect comes into play when exciton is confined in three spatial dimensions, resulting in a semiconductor having properties between its bulk form and discrete molecules. Theoretically, the decrease in the size SiC of QDs leads to an increase in the energy bandgaps due to quantum confinement. Likewise, the PL spectra is red shifted when the excitation wavelength increases in which the excitation energy decreases than their bandgap energy that can no longer excite the QDs regardless of SiC polytypes [69].

Furthermore, the surface defects of SiC can lead to similar behaviour as the quantum confinement effect. In other words, the dangling band, vacancies, and oxygen-related defects on the surface of SiC QDs may introduce localized energy within the

bandgap of the QDs which can lead to quantum confinement [67], [70]. In addition, more recent research discovered that while the emission PL peaks at short excitation wavelengths remain the same, indicating surface related luminescence, this shift in PL peaks only happens at longer excitation, suggesting quantum confinement effect with unique optical and electronic properties that have the potential to enhance the power conversion efficiency of solar cells as depicted in Figure 2.3 [63], [69], [71]. Further evidence shows that the emissions, which are polytype independent and always above energy bandgap is connected to surface defects rather than size-related quantum confinement [68], [72]. The surface termination has been proven to be impactful in making PL dependent on the type of solvent employed and preparation technique [73], [74], [75]. It should be noted that, despite having different crystal structures and band gaps, 3C, 4H, and 6H-SiC were found to have similar PL characteristics due to phase transformation from 4H or 6H into 3C during the ultrasonication process in the etching method [71], [73], [76] or from laser ablation method [77]. Nevertheless, rather than the polytypic shift, it was suggested that it is probably connected to band edge-impurity/defect level transitions [69]. Li *et al*., reported the fabrication of colloidal cubic 3C-SiC nanocrystals (QDs) in water and ethanol, in which both exhibited strong and above bandgap blue and blue-green emissions but showed different surface charges. The colloidal 3C-SiC QDs with water molecules indicate polar Si-terminated surfaces of cubic 3C-SiC nanocrystals. The results revealed the quantum confinement effect and surface charges of colloidal 3C-SiC QDs in water and ethanol, which play a great role in determining the distinct optical properties of the material [79].

Due to its strong chemical and photoluminescence stability, SiC NP is a very desirable option for optoelectronic applications. On top of that, SiC QDs were proven to be an effective material by significantly improving the characteristics of the solar

cells and increasing its stability, which can be explained by the exciton decay, by which electron passes through SiC QDs before going to substate coated with titanium dioxide (TiO_2) [79]. Recently, Benfadel *et al*., employed the use of SiC nanoparticles (NP) to formulate a nanocomposite layer for wavelength down-conversion, which was incorporated into polyvinyl alcohol (PVA) as a matrix that shows an improvement in spectral response with an increase in external quantum efficiency (EQE) in the order of 12.2 % when compared with material without SiC NP. Thus, the result as shown in **Figure 2.4** is indicative that the incorporation of SiC NP as wavelength down-conversion is beneficial to the improvement of the performance of obtained solar cells [27].

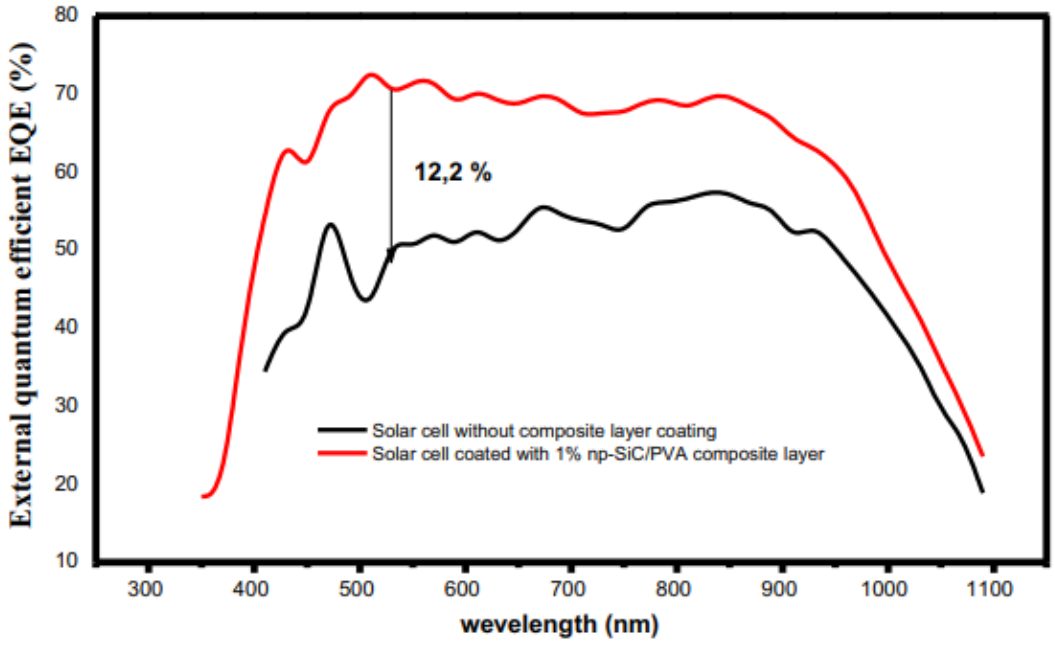

Figure 2.4 External Quantum Efficiency Spectra of a Solar Cell Without and With Deposition of the 1% NP 3C-SiC/ PVA Composite Layer [27]

The decrease in surface reflectance was also noticed after coating crystallite Si (c-Si) with a 3C-SiC luminescent down-shifting (LDS) layer, suggesting an antireflection coating property of the 3C-SiC. Upon exposure of 3C-SiC/PVA

composite layer deposited on c-Si to UV light illumination with an incident power of 170 W, the J-V curve showed an enhancement in photocurrent, which elaborates the conditions of the luminescent 3C-SiC nanocrystal. Hence, 3C-SiC LDS based can be employed to minimize the optical losses of c-Si based solar cells [14]

A cost-effectiveness and high-performance UV SiC thin film photodetectors with high response were fabricated by Aldalbahi *et al*. The fabricated SiC detectors seem to have stability and repeatability to a wide region of UV incident light (250 to 350 nm). The incident UV light of 250 nm with a power intensity of 2 mW/cm^2 produced photocurrent and responsivity of 55 μA and 0.18 A/W, which is almost 40 % higher in comparison with commercially available detectors [80]. Despite the advantages of colloidal SiC QDs, the physics behind luminescence property with the issue of complex surface state, structure, and dependency of surface termination such as -H and -OH on the nature of solvents used are still not yet fully understood [75], [81]. Moreover, the inability to precisely control the size of the NPS during the fabrication process may be one of the reasons why the exact source of PL in SiC QDs is still unknown[70]. In addition to understanding the underlying mechanism, more research and development of synthesis techniques are required to find more potential applications related to their optical property. For instance, colloidal SiC QDs can be incorporated into black Si (b-Si) for surface passivation to reduce thermalization losses and absorbance enhancement for photovoltaic applications.

2.3.1 Polytypes of SiC

More than 250 polytypes of SiC are known to exist as a polytypic material in the most common among them are 3C, 4H, and 6H. Several polytypes of SiC can be produced by stacking the tetrahedrally bonded bilayers of Si-C in different sequences. As seen in **Figure 2.5**, there are three types of sites known as A, B, and C, in arranging

the bilayers with each layer being normal to the c-axis. The direction to the Si-C double atomic layer is indicated by the c-axis. The three bilayers form distinct polytypes along the c-axis by forming a periodical sequence with repeating units along the c-axis [82].

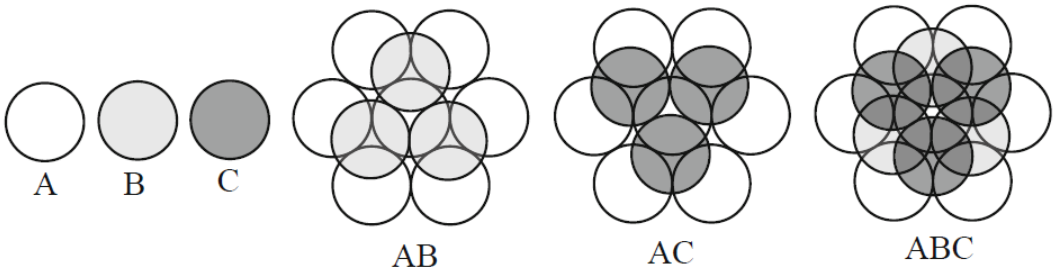

Figure 2.5 Three Types (A, B, C) of Si–C Bilayer Arrangement Along the c-axis (Stacking Direction) Through Close-Packed Spheres. The c-axis is Normal to the Paper Plane [82]

For instance, the 3C-SiC (β-SiC) with a face-centred cubic (fcc) lattice is named as zinc-blende structure. The stacking arrangement in 3C-SiC of the bilayers is ABCAB, where the letter ‘‘C’’ and “3” denote the cubic crystal structure and the number of bilayers in one repeating unit (ABC) respectively. The only cubic structure among the polytype is 3C-SiC, which forms at a low temperature [83]. 4H and 6H are wurtzite lattices (α-SiC) with a hexagonal closed pack (hcp) structure forming through the hexagonal stacking sequence ABCBABCB and ABCACBABCACB [72]. Similarly, the number attached to ‘‘H’’ (4 and 6) denotes the number of bilayers in one repeating unit. 4H and 6H can be formed at a temperature of 1700 °C [83]. There are many polymorphism modifications that arise owing to the small difference in energy between cubic and hexagonal structures. **Figure 2.6** depicts the Si–C double-atomic layers arrangement of 3 different types of polytypes [84].